Kinetics of the Quaternary Structure Change of Aspartate Transcarbamylase Triggered by Succinate, a Competitive Inhibitor†

Hirotsugu Tsuruta,*,‡ Patrice Vachette,§ Takayuki Sano,‖ Michael F. Moody,⊥ Yoshiyuki Amemiya,# Katsuzo Wakabayashi,∞ and Hiroshi Kihara▽

Stanford Synchrotron Radiation Laboratory, SLAC, P.O. Box 4349, MS 69, Stanford, California 94309-0210, LURE (CNRS/CEA/MESR), Bât 209d, Université Paris-Sud, F91405, Orsay Cedex, France, Department of Materials Science, Faculty of Science, Hiroshima University, Higashi-Hiroshima 734, Japan, School of Pharmacy, University of London, 29/39 Brunswick Square, London WC1N 1AX, UK, Photon Factory, National Laboratory for High Energy Physics, Tsukuba 305, Japan, Department of Biophysical Engineering, Faculty of Engineering Science, Osaka University, Toyonaka 560, Japan, and Physics Laboratory, Kansai Medical University, Hirakata, Osaka 573, Japan

Received April 4, 1994; Revised Manuscript Received June 14, 1994®

ABSTRACT: The quaternary structural change of *Escherichia coli* aspartate transcarbamylase (ATCase) was studied by time-resolved X-ray solution scattering following the binding of carbamoyl phosphate and of succinate, a competitive inhibitor of the natural substrate L-aspartate. Stopped-flow experiments at sub-zero temperatures in the presence of 30% ethylene glycol allowed us to monitor the evolution of the scattering pattern, including the characteristic scattering peak in an s (=2 sin θ/λ) range of 0.01–0.06 Å^{-1}. The inhibitor binding promotes a quaternary structure change from the T state toward the R state, and as expected for a simple ligand binding process, ATCase remains in the R state, unlike the physiological enzyme reaction [Tsuruta, H., et al. (1990) *FEBS Lett. 263,* 66–68]. After equilibrium had been established, the final scattering pattern was recorded. When the succinate concentration was sufficiently high, this pattern was the same as that given by ATCase saturated with the bisubstrate analogue *N*-phosphonoacetyl-L-aspartate (PALA). This implies that, under cryogenic conditions, succinate and carbamoyl phosphate promote the same quaternary structure change as PALA, which is in good agreement with the crystallographic studies of Gouaux and Lipscomb [Gouaux, J. E., & Lipscomb, W. N. (1988) *Proc. Natl. Acad. Sci. U.S.A. 85,* 4205–4208]. Scattering patterns recorded during the course of the structural transition were satisfactorily reproduced by a linear combination of the initial and final patterns, suggesting that there is no significant concentration of quaternary structure intermediates between the T and R states. This is consistent with a concerted structural transition of ATCase. The kinetic data yield the change of $\bar{R}$ (fraction of R structure) with time, from which the apparent rate constant, k_{app}, of the structure change is calculated. k_{app} is substantially larger at higher succinate concentrations, and this concentration dependence looks like the early stage of a sigmoidal curve. The $\bar{R}$ value evaluated for the final equilibrium patterns increases in a similar way, but it saturates at a lower succinate concentration than the rate constant. The two-state allosteric transition model, originally proposed by Monod et al. [Monod, J., Wyman, J., & Changeux, J. (1965) *J. Mol. Biol. 12,* 88–118], successfully accounts for both the kinetic (rate constant) and final static ($\bar{R}$) observations and allows estimates of the reaction parameters that characterize the allostery of ATCase. The reaction parameters thus obtained are not only self-consistent but also in good agreement with those obtained in other studies.

Aspartate transcarbamylase (ATCase[1]) is an allosteric enzyme that catalyzes the formation of carbamyl aspartate from carbamoyl phosphate and L-aspartate, the first committed step of the pyrimidine biosynthetic pathway of *Escherichia coli*. Like most allosteric proteins, ATCase is activated by substrate binding (homotropic effect) and is activated or inhibited by the nucleotide effectors ATP and CTP (heterotropic effect). Quaternary structure changes are believed to play a key role in the allosteric properties of oligomeric proteins like ATCase (Monod et al., 1965; Perutz, 1989). In support of this, a comparatively large quaternary structure change is found in ATCase by sedimentation velocity measurements (Gerhart & Schachman, 1968), solution X-ray scattering (Moody et al., 1979), and X-ray crystallography [Kantrowitz and Lipscomb (1988) and references therein].

We earlier demonstrated that time-resolved X-ray solution scattering is able to follow the quaternary structure changes of ATCase at low temperatures following binding of the natural substrates (Tsuruta et al., 1990). However, this physiological enzyme reaction may involve secondary effects caused by aspartate and the reaction product phosphate, which are known to promote a similar quaternary structure change (Gouaux & Lipscomb, 1989). Here we avoid this complication by replacing substrates with ligands (carbamoyl phosphate and

† This work was carried out under Photon Factory Proposals 88-060, 90-063, and 92-116. Facilities were also provided by SSRL, which is funded by the U.S. Department of Energy, Office of Basic Energy Sciences, with further support provided by the Office of Health and Environmental Research. The SSRL Biotechnology Program is supported by the National Institutes of Health, Biomedical Research Technology Program, National Center for Research Resources. H.T. received a postdoctoral fellowship from the Japan Society for the Promotion of Science and a related grant from the Ministry of Education, Science and Culture, Japan. M.F.M. received an EMBO short-term fellowship.

‡ Stanford Synchrotron Radiation Laboratory.
§ Université Paris-Sud.
‖ Hiroshima University.
⊥ University of London.
National Laboratory for High Energy Physics.
∞ Osaka University.
▽ Kansai Medical University.

® Abstract published in *Advance ACS Abstracts,* August 1, 1994.

[1] Abbreviations: ATCase, aspartate transcarbamylase (or aspartate carbamoyltransferase); PALA, *N*-phosphonoacetyl-L-aspartate.

0006-2960/94/0433-10007$04.50/0

succinate) that undergo no catalytic reactions.

Succinate is an inhibitor that competitively binds to the same site as L-aspartate (Jacobson & Stark, 1973, 1975). Succinate and carbamoyl phosphate generate a quaternary structure change (Gerhart & Schachman, 1968; Howlett et al., 1977; Hervé et al., 1985), yielding a structure that is very similar to that observed in ATCase saturated with the transition state analogue PALA (Gouaux & Lipscomb, 1988). Here we present a time-resolved X-ray scattering study of the quaternary structure change produced by this inhibitor binding and describe a two-state allosteric transition model that accounts for the kinetics of the structural change.

EXPERIMENTAL PROCEDURES

Carbamoyl phosphate (Wako Chemicals) was purified by recrystallization from ice-cold 50% ethanol (Gerhart & Pardee, 1962) and freeze-dried. All solutions containing carbamoyl phosphate were kept frozen to minimize hydrolysis and were used in the X-ray scattering experiments within a few days. Monosodium succinate (Nakarai) was of certified grade. Analytical grade ethylene glycol (Wako or Nakarai) was used as an antifreeze in a 30% volume ratio. Other chemicals were either analytical or certified grade.

The *E. coli* strain 1510G4PYRF$^{\pm}$ with a pBh104 plasmid was obtained from Dr. G. Hervé (then at the Institute d'Enzymologie, CNRS, Gif-sur-Yvette, France). It was cultured in 100 or 150 L at the Institute for Protein Research, Osaka University. The wet cell pellet was kept frozen at −20 °C until enzyme purification (Gerhart & Holoubek, 1967). The purified enzyme was first dissolved in the buffer solution (pH 8.3) containing 80 mM Tris, 90 mM borate, 1 mM ethylenediaminetetraacetate, 0.2 mM 2-mercaptoethanol, and 0.2 mM phenylmethanesulfonyl fluoride and then concentrated centrifugally using a Centriflo CF-25A (Amicon) up to approximately 100 mg/mL. Before the X-ray scattering measurements, the concentrated enzyme solution was dialyzed for at least 36 h against the buffer solution containing 30% (v/v) ethylene glycol. The enzyme concentration was determined spectrophotometrically using an extinction coefficient $E(1\%, 1\text{ cm}) = 5.9$ at 280 nm (Gerhart & Holoubek, 1967).

Stopped-flow X-ray scattering experiments were performed on beam line 15A at the Photon Factory, National Laboratory for High Energy Physics, Tsukuba, Japan. The 2.5-GeV positron storage ring was operated at a ring current of 200–350 mA, with an injection every 12 or 24 h. A short open-air ionization chamber was placed just upstream of the sample to monitor the intensity of the incident X-ray beam, whose flux was typically $(0.7–1.3) \times 10^{11}$ photons/s and which was 1.5 mm high and 2.5 mm wide at the specimen. Scattered X-rays were recorded by a one-dimensional position-sensitive proportional counter (Rigaku, Japan) placed 0.9–1.2 m from the specimen. The detector had an effective length of 170 mm and 512 detection channels. Details of the small-angle scattering/diffraction camera system are given elsewhere (Amemiya et al., 1983; Wakabayashi & Amemiya, 1991). In addition to the regular beam-stop, the central part of the detector (where scattered X-rays from the concentrated enzyme are very strong) was covered with a lead plate in order to keep the total counting rate, which was approximately $(1.0–1.8) \times 10^4$ counts/s, well below the limit of the detection system. We show the scattering patterns as a function of the scattering vector $s = 2 \sin \theta/\lambda$, where 2θ is the scattering angle and λ is the X-ray wavelength (1.50 Å).

Fast mixing was performed using a sub-zero stopped-flow apparatus (Tsuruta et al., 1989) with a dead time below 10 ms. The inhibitor reaction was initiated by mixing equal volumes (0.1 mL) of (i) an enzyme solution (74 mg/mL) and (ii) a solution containing carbamoyl phosphate and succinate (at various concentrations). Immediately after mixing, 95 time-resolved scattering patterns were recorded, usually with increasing exposure times (e.g., 25 patterns of 0.1 s each and then 25 patterns of 0.2 s each and so on), so that a single set of time-resolved measurements covered both the fast initial events and the slower ones near equilibrium. Each experiment was repeated 25 times except those in Figure 5, which were repeated 7–9 times. All sequences of scattering patterns were averaged after inspection for any artifact and scaling to the intensity of the incident X-ray beam. A final (equilibrium) scattering pattern was recorded, for 300 or 600 s, 6 min or more after mixing. All experiments were performed at either −8 or −11 °C in the presence of 30% (v/v) ethylene glycol.

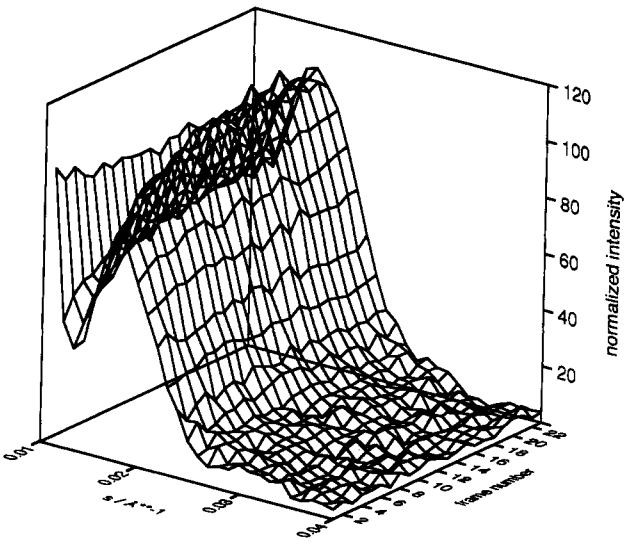

FIGURE 1: Time-resolved X-ray scattering patterns recorded during the succinate reaction. At −11 ± 0.8 °C in the presence of 30% (v/v) ethylene glycol, ATCase solution (74 mg/mL) was mixed with a substrate solution containing 80 mM carbamoyl phosphate and 20 mM succinate in a 1:1 ratio. Scattering patterns were then collected successively as described in the text. The experiment was repeated 25 times. Equivalent sets of 25 time-resolved patterns were combined together, and then several consecutive patterns were averaged to give 4 s interval patterns. The intensities are plotted every 0.001 Å^{-1} for clarity in the s range 0.011–0.040 Å^{-1}.

RESULTS

Figure 1 shows a typical series of time-resolved scattering patterns following the binding of carbamyl phosphate and succinate. Immediately after mixing, the pattern is close to that of unligated ATCase, i.e., the T quaternary structure. As the reaction proceeds, the pattern progressively more closely resembles that of ATCase saturated with succinate and carbamoyl phosphate (or with PALA), i.e., the R structure.

The initial scattering pattern recorded in the presence of D-aspartate (curve 1, Figure 2) is identical, within experimental error, to that of the unligated protein. This represents the T structure, since such scattering patterns agree with one calculated from the crystal structure of the T form ATCase (Altman et al., 1982). D-Aspartate was added when recording curve 1 so as to bring the electron density of the solvent close to that in the time-resolved measurements. D-Aspartate also serves as a control for the nonspecific binding of aspartate. The first scattering pattern, which is an average of a large number of successively recorded time-resolved patterns after mixing, shows a small but detectable difference from the initial pattern (curve 3, Figure 2). It indicates that the very first part of the reaction *could not* be recorded with good statistics.

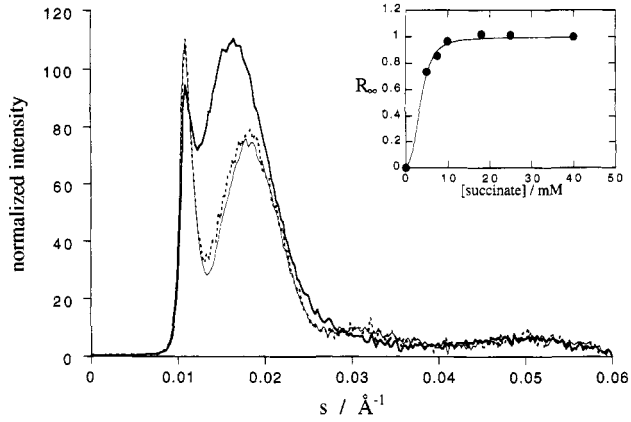

FIGURE 2: Curve 1 (thin solid line): Scattering pattern in the presence of 40 mM carbamoyl phosphate and 10 mM D-aspartate. Curve 2 (thick solid line): Final scattering pattern (same conditions as in Figure 1) . Curve 3 (dotted line): Initial scattering pattern from a time-resolved experiment (0–4 s after mixing). The first two curves were recorded with a 600-s exposure in the stopped-flow mixer, as in the time-resolved measurement. Curve 3 is the first pattern from the time-resolved data shown in Figure 1. Curve 1 was taken as the T pattern and curve 2 as the R pattern in the linear combination fit of the time-resolved data. Note that the s range less than 0.01 Å^{-1} was covered by a lead plate in order to reduce the total counting rate. Inset: Plot of $\bar{R}_\infty$ versus succinate concentration expressed in fractional change of the integrated intensity over the scattering peak. The solid curve is a fit with the parameters K_R = 2.4 mM, c = 0.12, and L_0 = 80.

More precisely, the first pattern corresponds to a linear combination with 10% R state. In the presence of low concentrations of succinate, the final scattering pattern depends on succinate concentration. Beyond about 10 mM succinate (in the presence of 44 mM carbamoyl phosphate), this scattering pattern shows no further detectable change (Figure 2, inset) and is very close to the pattern observed in the presence of saturating PALA; ATCase is therefore presumed to be in the R quaternary structure.

Intermediary Structure. The present study is mainly aimed at detecting, during the course of the transition, the presence of an intermediary structure different from the initial and final structures. Any scattering pattern can be represented by **I**, a vector whose components are the numbers of X-ray photons scattered into different detector channels. At an intermediate time t of the binding reaction, each pattern $\mathbf{I}_t$ can be expressed as a linear combination of the T and R patterns ($\mathbf{I}_0$ and $\mathbf{I}_\infty$, respectively, shown in Figure 2):

$$\mathbf{I}_t = (1 - \bar{R}_t)\mathbf{I}_0 + \bar{R}_t\mathbf{I}_\infty$$

$\bar{R}_t$ can be determined by a least-squares fit to the two standard patterns $\mathbf{I}_0$ and $\mathbf{I}_\infty$; i.e., $\bar{R}_t = (\mathbf{I}_t - \mathbf{I}_0)(\mathbf{I}_\infty - \mathbf{I}_0)/|\mathbf{I}_\infty - \mathbf{I}_0|^2$. The adequacy of this approximation can be estimated by calculating the residual:

$$\rho_t = \mathbf{I}_t - \{(1 - \bar{R}_t)\mathbf{I}_0 + \bar{R}_t\mathbf{I}_\infty\}$$

The upper sections of Figure 3 show such residuals. They appear to be merely noise, since they show none of the smooth dependence on s that is characteristic of ATCase scattering patterns such as $\mathbf{I}_0$ or $\mathbf{I}_\infty$.

Kinetic Analysis. The kinetics of the reaction can be determined by the time dependence of $\bar{R}_t$ as shown in Figure 4A for a succinate concentration of 10 mM. Alternatively, one can use the simple procedure of following the time dependence of the integral under certain peaks, as in previous studies (Tsuruta et al., 1990; Kihara et al., 1987). The corresponding curve is shown in Figure 4B. However, it is desirable to minimize the contribution to the integral from those parts of spectrum where there is the least change. This can be done by multiplying the integrand by a suitable filter. Such a filter is $\Delta\mathbf{I} = \mathbf{I}_\infty - \mathbf{I}_0$, since it is small where the spectrum shows little change. It is therefore better to replace the simple integral $(\mathbf{1})(\mathbf{I}_t)$ ($\mathbf{1}$ is a constant vector) by $(\Delta\mathbf{I})\mathbf{I}_t = r_t$. As might be expected, r_t is closely related to $\bar{R}_t$. Indeed, using the least-squares formula for $\bar{R}_t$,

$$\bar{R}_t = (\mathbf{I}_t - \mathbf{I}_0)(\mathbf{I}_\infty - \mathbf{I}_0)/|\mathbf{I}_\infty - \mathbf{I}_0|^2 = (\mathbf{I}_t - \mathbf{I}_0)(\Delta\mathbf{I})/|\Delta\mathbf{I}|^2 = a(\Delta\mathbf{I})\mathbf{I}_t - b = ar_t - b$$

where $a = 1/|\Delta\mathbf{I}|^2$ and $b = \mathbf{I}_0(\Delta\mathbf{I})/|\Delta\mathbf{I}|^2$ depend only on the T and R patterns. Figure 4C shows a plot of r_t against t, using the same data plotted in Figure 4A,B. The three curves, expressing the kinetics of the reaction, are very similar, and all three are approximated adequately by a single exponential, within experimental errors. They yield very similar values for the apparent rate constant (k_{app}) of the T to R transition

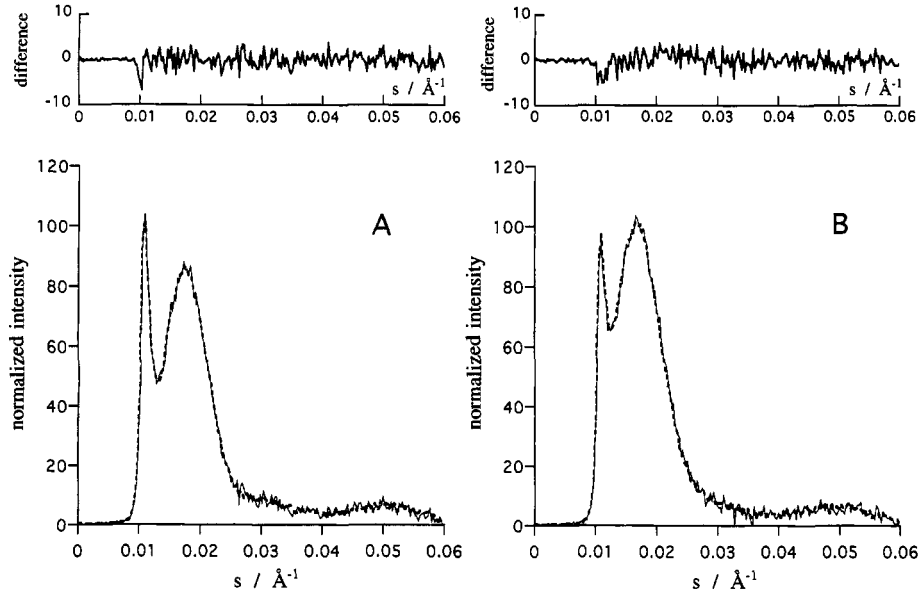

FIGURE 3: Time-resolved patterns along with corresponding linear combination patterns: Solid curve, time-resolved pattern; broken curve, best least-squares fit using a linear combination of T and R patterns. The difference between the two curves is shown in the upper part of the figure. The fraction of the R structure, $\bar{R}$, was determined to be 0.392 ± 0.006 for A (at 8–12 s) and 0.799 ± 0.004 for B (at 44–48 s) by a nonlinear least-squares fit in the s range 0.012–0.04 Å^{-1}.

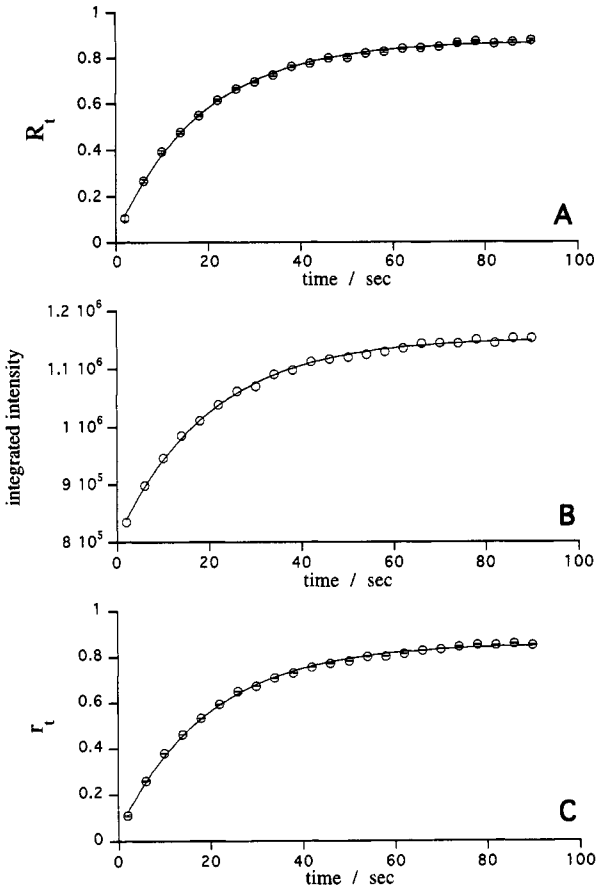

FIGURE 4: Evolution of the structural change shown for the different quantities: A, $\bar{R}$; B, integrated intensity over the s range 0.012–0.026 Å^{-1}; C, $\bar{r}$. Evaluated apparent rate constants are (5.25 ± 0.10) × 10^{-2} s^{-1} (A), (4.99 ± 0.11) × 10^{-2} s^{-1} (B), and (5.05 ± 0.11) × 10^{-2} s^{-1} (C), respectively.

in the presence of 10 mM succinate: (5.25 ± 0.10) × 10^{-2} s^{-1} (A), (4.99 ± 0.11) × 10^{-2} s^{-1} (B), and (5.05 ± 0.11) × 10^{-2} s^{-1} (C), respectively. Note that k_{app} is not a true constant since it depends on the succinate concentration (Figure 5). This dependence and the plot of $\bar{R}_\infty$ versus succinate concentration (Figure 2, inset) can be interpreted by the model of Monod et al. (1965) (Scheme 1).

This model assumes that an allosteric protein comprising n subunits (here $n = 6$) is either in a T state, which has a lower affinity for ligands, or in an R state, which has a higher affinity. More specifically, each subunit in the R state binds one succinate molecule, M, with a dissociation constant, K_R, independent of the state of ligation. In the same way, the T state has a dissociation constant $K_T = K_R/c$, where c should be a constant less than 1. We further assume that the rates of the structural transitions are far slower than the on-/off-rates of carbamoyl phosphate or succinate binding. Finally, we reduce the number of kinetic parameters of the model by assuming that the R → T conversion rates are independent of the state of ligation ($k_{-0} = k_{-1} = ... = k_{-6}$), which results in $k_{-0} = ck_1 = c^2k_2 = ... = c^6k_6$. Provided that succinate is always present in such excess that its concentration is effectively constant, these simplifications allow us to solve the kinetic equations (Eckfeldt et al., 1970)[2], giving

$$k_{app} = k_0\left(\frac{1 + [M]/K_R}{1 + c[M]/K_R}\right)^6 + k_{-0} \qquad (1)$$

When the initial values were varied over meaningful ranges (1 mM < K_R < 10 mM; 0.02 < c < 0.3; 0.001 < k_{-0} < 0.1; 10 < L_0 < 1000), a nonlinear least-squares fit of the equation to the experimental data in Figure 5 yields parameter values in the following ranges: 2 mM < K_R < 5 mM; 0.06 < c < 0.13; 3 × 10^{-5} s^{-1} < k_0 < 3 × 10^{-4} s^{-1}; and $k_{-0} \approx 5 \times 10^{-2}$ s^{-1}. The values of K_R and c are within the ranges found by steady state kinetics [$c = K_R/K_T = 0.05$: Gibbons et al. (1976) and Howlett et al. (1977); K_R = 1.4 mM: Suter and Rosenbusch (1976)]. The ratio of the rate constants $L_0 = k_{-0}/k_0$ is found to be in the range of several hundred, qualitatively in good agreement with the fact that ATCase is essentially in the T state in the absence of succinate.

[2] Notation of the rate constants is reversed in this reference.

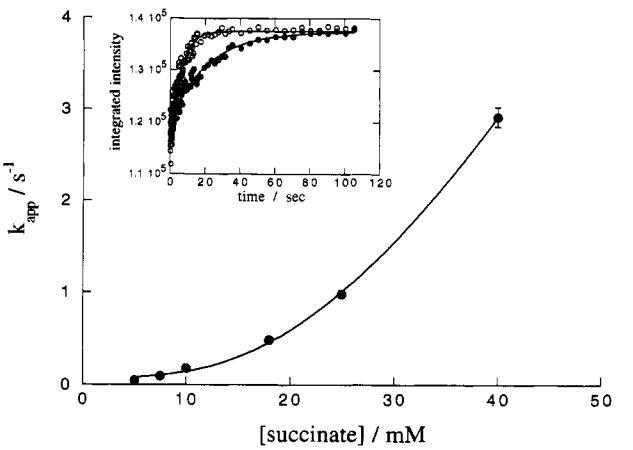

FIGURE 5: Succinate concentration dependence of the rate of the structural change. Stopped-flow X-ray scattering experiments were performed as described in the text at –8 °C in the presence of 30% ethylene glycol at a carbamoyl phosphate concentration of 44 mM (after mixing). The apparent rate constant (inverse time constant) is plotted versus the final succinate concentration. The solid curve is the calculated fit by iterative nonlinear least-squares based on the two-state allosteric transition model described in the text with the evaluated parameters: K_R = 3.5 mM; c = 0.1; $k_0 = 5 \times 10^{-2}$ s^{-1}; and $k_{-0} = 9 \times 10^{-5}$ s^{-1}. The inset shows the kinetics of the structural change expressed in integrated intensity (s range 0.0143–0.0226 Å^{-1}) recorded at 5 mM (●) and 10 mM final succinate (○). The least-squares fit gives apparent rate constants (4.74 ± 0.34) × 10^{-2} s^{-1} for the former and (1.77 ± 0.09) × 10^{-1} s^{-1} for the latter.

Scheme 1

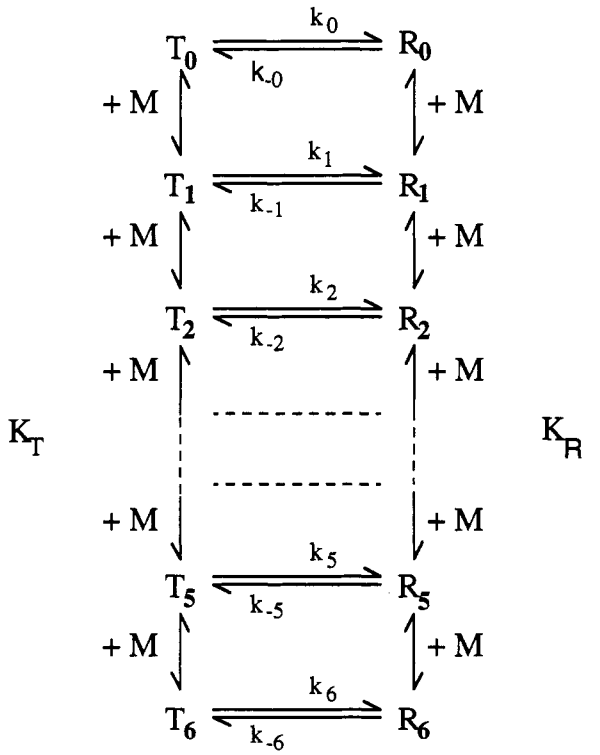

With the same model, the saturation curve of $\bar{R}_\infty$ in Figure 2 can be expressed as

$$\bar{R}_\infty = \sum_{i=0}^{6} R_i \Big/ \sum_{i=0}^{6} (R_i + T_i) = (1 + [M]/K_R)^6/[L_0(1 + c[M]/K_R)^6 + (1 + [M]/K_R)^6]$$

A least-squares fit of the experimental result (Figure 2, inset) gives K_R values between 2 and 4 mM, a c of about 0.1, and L_0 on the order of 100, which are compatible with our previous determinations of the kinetic data.

DISCUSSION

Stopped-flow X-ray scattering allows one, in principle, to determine important aspects of the structures reacting and even of intermediate forms. At the existing synchrotron radiation facilities, time-resolved solution X-ray scattering measurements on biological macromolecules can be performed, with satisfactory statistics, in the time regime of seconds. Faster processes can also be studied if cryotechniques are used to slow down the reaction. The resulting kinetic scattering patterns can be interpreted in two ways, i.e., as distinct structural snapshots of the mixture or as a kinetic portrait of the time evolution of the binding process. We will discuss these three issues separately.

Stopped-Flow Measurements at Sub-Zero Temperatures. A stopped-flow rapid mixer has been designed specifically for use at sub-zero temperatures in the presence of cryosolvent (Tsuruta et al., 1989). Under these conditions, the quaternary structural change becomes slow enough to be monitored by X-ray scattering with reasonable counting statistics (Tsuruta et al., 1990), after about 20 repeats for each measurement. X-ray scattering patterns of ATCase recorded at −10 °C with 30% ethylene glycol, both in the absence of substrate and in the presence of saturating PALA, are identical to those recorded in standard conditions (no ethylene glycol at 25 °C) (Tsuruta et al., 1993). The enzyme also retains significant catalytic activity (Narumi, personal communication). Thus, the cryogenic conditions used for the stopped-flow experiments apparently do not alter the quaternary structure and enzymatic properties of ATCase, despite their probable effects on binding or rate constants.

Structures. The scattering curves recorded during the reaction can all be approximated satisfactorily by some linear combination of the T and R scattering curves. This is shown by calculating the residuals, i.e., the differences between the calculated and experimental curves. If a third scattering component were needed, then these residuals would have the consistent, smooth modulation characteristic of X-ray scattering curves. Any such modulation lies below the noise level of the residuals. This implies that if any additional structural forms are present, they either must give a scattering curve that is a linear combination of R and T curves or else must be present at so low a concentration that their contribution to the overall scattering is undetectable. The first alternative would be true of forms that are just minor variants of the T or R states, resulting perhaps from some slight structural flexibility. The second alternative is almost certainly true for some intermediates; any transition delayed by a high activation energy barrier [which is true for ATCase: Kihara et al. (1984)] can have only a small concentration of forms in the process of crossing that barrier. Unfortunately, it will be very difficult to obtain any experimental evidence concerning their structures.

Previous hydrodynamic measurements, such as the sedimentation coefficient (Gerhart & Schachman, 1968; Howlett et al., 1977; Werner & Schachman, 1989), were shown to agree with a two-state model for ATCase. Our least-squares analysis of X-ray scattering patterns provides a much more stringent test of this hypothesis. Furthermore—and this is beyond the reach of hydrodynamic methods—X-ray scattering gives information about the structural transition's kinetics, to which we now turn.

Kinetics. The time course of the structural changes, expressed as a plot of r_t or $\bar{R}_t$ against t, fits a single-exponential curve within experimental error. This may result from the superimposition of the different structural transitions whose rate constants are too close to be resolved. A few assumptions were made to linearize the simultaneous differential equations, so as to obtain a simple analytical expression for the apparent rate constant, k_{app}, which only depends on a small number of parameters (eq 1). It is of interest to examine briefly the validity of these hypotheses. The assumption that the on-/off-rates of substrate binding are fast compared to the rates of the structural transitions obviously is not a very restrictive one. The hypothesis regarding the constancy of substrate concentration through the structural transition is valid for most of the data presented. Finally, the assumption that all rate constants of the R to T transitions, k_{-i}, are equal regardless of the state of ligation is purely arbitrary and simply aimed at a drastic reduction in the number of parameters before attempting to fit our experimental results. Otherwise, such a complex set of coupled structural reactions cannot be modeled in a unique way, and the values derived for the parameters should be given only qualitative significance. However, it is again worth noting the agreement between the orders of magnitude of the values derived for the equilibrium parameters, K_R, c, and L_0, and the values that can be found in the literature. Thus, our kinetic data fit the model of Monod et al. (1965), as well as (presumably) a large number of more complicated models.

One can also use more realistic assumptions for the rate constants. For instance, bound substrates might be expected not only to shift the T ⇔ R equilibrium toward R but also to act on the kinetics of the reactions by facilitating the T to R transition and slowing down the reverse R to T transition, so that $k_{-i} > k_{-j}$, $1 \le i < j \le 6$. The simple relationship $k_{-i} = k_{-0}/(i + 1)$, which roughly corresponds to a proportional effect of bound substrate on the rate constant with the associated relationship $k_i = k_0/[(i + 1)c^i]$ for the reverse rates, gives the following expression for k_{app}:

$$k_{app} = \frac{K_R}{7[M]}((1 + [M]/K_R)^7 - 1) \times \left(\frac{k_0}{(1 + c[M]/K_R)^6} + \frac{k_{-0}}{(1 + [M]/K_R)^6}\right) \quad (2)$$

A least-squares fit to the data of Figure 5 gives the following ranges for the parameters: 2 mM $< K_R <$ 4 mM; 4×10^{-5} s^{-1} $< k_0 < 7 \times 10^{-4}$ s^{-1}; $0.06 < c < 0.11$; 0.2 s^{-1} $< k_{-0} <$ 0.4 s^{-1}. The values of the equilibrium parameters K_R and c are the same as those previously described. The rate constant k_{-0} is about an order of magnitude larger, as one expects since it was made to be the largest R to T constant.

Kinetic studies of the interaction of ATCase with succinate in the presence of saturating carbamyl phosphate were performed more than 20 years ago by Hammes and Wu (1971) using the temperature-jump method. They used the absorption change of a pH indicator to monitor the pH change accompanying the relaxation process following a temperature jump of about 7 °C. In this article, Hammes and Wu mention their following of succinate binding to ATCase. In fact, they

most probably observed substrate release from the active site since they increased the temperature, while the electrostatic interactions mainly responsible for the binding of charged substrates to the active site tend to decrease with temperature. Furthermore, the T to R quaternary structure transition has been shown to be exothermic (Knier & Allewell, 1978; Shrake et al., 1981), so that an increase in temperature is expected to shift the equilibrium toward the T structure. Finally, X-ray scattering measurements recently have been performed as a function of temperature on solutions of ATCase containing saturating carbamoyl phosphate and subsaturating succinate. The scattering pattern of ATCase shifts toward the T pattern as the temperature is increased (Fetler et al., unpublished observation). Thus, we can with confidence interpret the temperature-jump (T-jump) measurements of Hammes and Wu (1971) as being associated with the relaxation of a fraction of the enzyme population from R to T.

The variation of k_{app} with succinate concentration observed by stopped-flow X-ray scattering (see Figure 5) is at variance with that observed by T-jump [see Figure 3 in Hammes and Wu (1971)]. Hammes and Wu see a marked decrease in k_{app}, which levels off at high succinate concentration, while we observe just the opposite behavior. These need not be incompatible results. For the sake of clarity, let us consider the global equilibrium between T and R, which implies all of the T and R forms regardless of their state of ligation, with associated overall rate constants k_+ and k_-. The T-jump experiment, which follows the relaxation of the solution after the equilibrium has been perturbed, yields the apparent rate constant $k_{app} = k_+ + k_-$, with $k_-/k_+ = [T]/[R]$ at equilibrium. Adding 1 to both sides and inverting gives $k_+/k_{app} = [R]/([T] + [R])$, so that k_+ is proportional to $k_{app}[R]$. On the other hand, the stopped-flow experiment converts the solution, originally wholly in T, entirely to R, and the apparent rate constant is dominated by the contribution from k_+, the rate of the T $\rightarrow$ R reaction. Since [R] rises as a sigmoid curve with [succinate], the product $k_{app}[R]$, which is proportional to k_+, could rise with [succinate], as we find, even though k_{app} falls with [succinate], as found by Hammes and Wu (1971). The same rationale applies to the more complex set of simultaneous equilibria. Thus, it probably is not necessary to invoke the differences in experimental conditions (different concentrations and temperatures) and the presence of cryosolvent in our stopped-flow experiments.

Time-resolved X-ray scattering measurements thus allow us to probe directly the quaternary structure distribution of an enzyme solution and its evolution following a perturbation. The results of both the structural and the kinetic analyses of our data give strong support to the view of a concerted transition between two quaternary structures for ATCase upon succinate binding. Further experiments devoted to the effect of the nucleotide allosteric effectors on the transition with the physiological substrate aspartate will be presented elsewhere.

ACKNOWLEDGMENT

The authors thank Drs. M. Sato and H. Yamaguchi, Institute for Protein Research, Osaka University, for their help in large scale *E. coli* fermentation and Prof. J. Janin for fruitful discussions. H.T. thanks Dr. H. Bellamy, SSRL, for final proofreading.

REFERENCES

Altman, R. B., Ladner, J. E., & Lipscomb, W. N. (1982) *Biochem. Biophys. Res. Commun. 108*, 592–595.

Amemiya, Y., Wakabayashi, K., Hamanaka, T., Wakabayashi, T., Matsushita, T., & Hashizume, H. (1983) *Nucl. Instrum. Methods 208*, 471–477.

Eckfeldt, J., Hammes, G. G., Mohr, S. C., & Wu, C.-W. (1970) *Biochemistry 9*, 3353–3362.

Gerhart, J. C., & Holoubek, H. (1967) *J. Biol. Chem. 242*, 2886–2892.

Gerhart, J. C., & Schachman, H. K. (1968) *Biochemistry 7*, 538–552.

Gibbons, I., Ritchey, J. M., & Schachman, H. K. (1976) *Biochemistry 15*, 1324–1330.

Gouaux, J. E., & Lipscomb, W. N. (1988) *Proc. Natl. Acad. Sci. U.S.A. 85*, 4205–4208.

Gouaux, J. E., & Lipscomb, W. N. (1989) *Proc. Natl. Acad. Sci. U.S.A. 86*, 845–848.

Hammes, G. G., & Wu, C.-W. (1971) *Biochemistry 10*, 1051–1057.

Hervé, G., Moody, M. F., Tauc, P., Vachette, P., & Jones, P. T. (1985) *J. Mol. Biol. 185*, 189–199.

Howlett, G. J., & Schachman, H. K. (1977) *Biochemistry 16*, 5077–5083.

Howlett, G. J., Blackburn, M. N., Compton, J. G., & Schachman, H. K. (1977) *Biochemistry 16*, 5091–5099.

Jacobson, G. R., & Stark, G. R. (1973) in *The Enzymes, 3rd Ed., Vol. 9*, (Boyer, P. D., Ed.) pp 225–308, Academic Press, New York.

Jacobson, G. R., & Stark, G. R. (1975) *J. Biol. Chem. 250*, 6852–6860.

Kantrowitz, E. R., & Lopscomb, W. N. (1988) *Science 241*, 669–674 .

Kihara, H., Takahashi-Ushijima, E., Amemiya, Y., Honda, Y., Vachette, P., Tauc, P., Barman, T. E., Jones, P. T., & Moody, M. F. (1987) *J. Mol. Biol. 198*, 745–748.

Knier, B. L., & Allewell, N. M. (1978) *Biochemistry 17*, 784–790.

Monod, J., Wyman, J., & Changeux, J. (1965) *J. Mol. Biol. 12*, 88–118.

Moody, M. F., Vachette, P., & Foote, A. M. (1979) *J. Mol. Biol. 133*, 517–532.

Newell, J. O., Markby, D. W., & Schachman, H. K. (1989) *J. Biol. Chem. 264*, 2476–2481.

Perutz, M. F. (1989) *Q. Rev. Biophys. 22*, 139–236.

Shrake, A., Ginsburg, A., & Schachman, H. K. (1981) *J. Biol. Chem. 256*, 5005–5015.

Suter, P., & Rosenbusch, J. P. (1976) *J. Biol. Chem. 251*, 5986–5991.

Tsuruta, H., Nagamura, T., Kimura, K., Igarashi, Y., Kajita, A., Wang, Z.-X., Wakabayashi, K., Amemiya, Y., & Kihara, H. (1989) *Rev. Sci. Instrum. 60*, 2356–2358.

Tsuruta, H., Sano, T., Vachette, P., Tauc, P., Moody, M. F., Wakabayashi, K., Amemiya, Y., Kimura, K., & Kihara, H. (1990) *FEBS Lett. 263*, 66–68.

Tsuruta, H., Vachette, Sano, T., Moody, M. F., Amemiya, Y., Wakabayashi, K., & Kihara, H. (1994) in *Synchrotron Radiation in Biosciences* (Sakabe, N., Ed.) Oxford University Press, Tokyo (in press).

Wakabayashi, K., & Amemiya, Y. (1991) in *Handbook on Synchrotron Radiation* (Ebashi, S., Koch, M., & Rubenstein, E., Eds.) pp 597–678, Elsevier Science Publishers/North-Holland, Amsterdam.

Werner, W., & Schachman, H. K. (1989) *J. Mol. Biol. 206*, 221–230.